JCI The Journal of Clinical Investigation

Keratinocyte-derived microvesicle particles mediate Ultraviolet B radiation induced systemic immunosuppression

Langni Liu, … , R. Michael Johnson, Jeffrey B. Travers

J Clin Invest. 2021. https://doi.org/10.1172/JCI144963.

Research In-Press Preview Dermatology Immunology

Graphical abstract

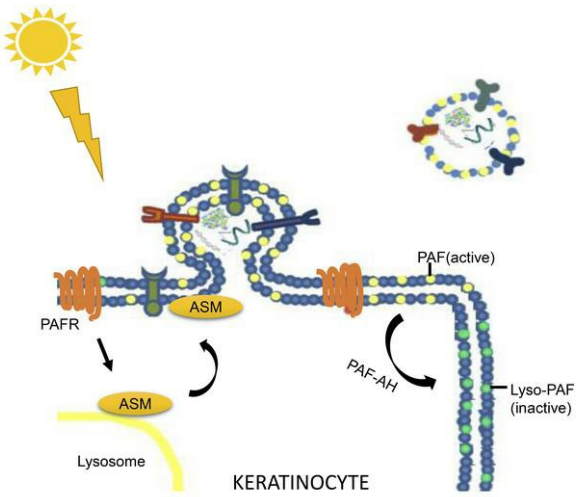

Keratinocyte-derived microvesicle particles mediate Ultraviolet B radiation induced systemic immunosuppression

Langni Liu [1], Azeezat A. Awoyemi[1], Katherine E. Fahy [1], Pariksha Thapa[1], Christina Borchers[1], Benita Wu[1], Cameron McGlone[1], Benjamin Schmeusser[1], Zafer Sattouf, Craig A. Rohan[1,2], Amy R. Williams[1], Elizabeth E. Cates[1], Christina Knisely[1], Lisa E. Kelly[1], Ji C. Bihl[1], David R. Cool[1], Ravi P. Sahu[1], Jinju Wang[1], Yanfang Chen[1], Christine M. Rapp[1], Michael G. Kemp[1], R. Michael Johnson[3], and Jeffrey B. Travers[1,2,4*].

Departments of [1]Pharmacology & Toxicology, and [2]Dermatology, [3]Plastic Surgery, Wright State University, Dayton OH.

[4]The Dayton V.A. Medical Center, Dayton, OH.

[*]Corresponding author:

Jeffrey B. Travers, M.D., Ph.D. Wright State University Department of Pharmacology & Toxicology, Dayton OH. jeffrey.travers@wright.edu

Phone: 937-775-2463

Fax: 937-775-7221

ORCIDs: 0000-0001-8069-6711 (L.L.);0000-0002-0312-7635 (A.A.A.); 0000-0002-7368-2589 (P.T.); 0000-0003-2404-1782 (J.C.B.); 000-0003-1210-7676 (J.W.), 0000-0001-8203-0745 (M.G.K), 0000-0003-4358-5056 (R.M.J.); 0000-0001-7232-1039 (J.B.T.).

Running title: *UVB generates PAF-containing microvesicles*

ABSTRACT

A complete carcinogen, Ultraviolet B radiation (290-320 nm; UVB), is the major cause of skin cancer. UVB-induced systemic immunosuppression that contributes to photocarcinogenesis is due to the glycerophosphocholine-derived lipid mediator Platelet-activating factor. A major question in photobiology is how UVB radiation, which only absorbs appreciably in the epidermal layers of skin, can generate systemic effects. UVB exposure and PAF Receptor (PAFR) activation in keratinocytes induce large amounts of microvesicle particle (extracellular vesicles 100-1000nm; MVP) release. MVPs released from skin keratinocytes in vitro in response to UVB (UVB-MVP) are dependent upon the keratinocyte PAFR. The present studies used both pharmacologic and genetic approaches in cells and mice to determine that both the PAFR and enzyme acid sphingomyelinase (aSMase) were necessary for UVB-MVP generation. Discovery that the calcium-sensing receptor is a keratinocyte-selective MVP marker allowed us to determine that UVB-MVP leaving the keratinocyte can be found systemically in mice and in human subjects following UVB. Moreover, UVB-MVP contain bioactive contents including PAFR agonists which allow them to serve as effectors for UVB downstream effects, in particular UVB-mediated systemic immunosuppression.

Introduction

Ultraviolet B radiation (290-320 nm; UVB), is both a mutagen and immunosuppressant and is a primary cause of skin cancer (1, 2). UVB-induced systemic immunosuppression is due to the glycerophosphocholine-derived lipid mediator Platelet-activating factor (PAF) in a process involving cyclooxygenase-2-derived prostaglandins and histamine/chemokine-regulated cell chemotaxis promoting mast cell migration to draining lymph nodes where they activate regulatory T (Treg) and potentially regulatory B cells, which contributes to photocarcinogenesis (3-7). Though this UVB-mediated systemic immunosuppressive pathway has been characterized, a major question which remains is how metabolically labile PAF agonists leave the epidermis.

Formed in response to diverse stressors, subcellular microvesicle particles (MVP) which form from the plasma membrane have been demonstrated to transport various bioactive substances (8, 9). Recent studies have implicated MVP as potential effectors for UVB. In particular, UVB irradiation of the keratinocyte-derived human cell line HaCaT as well as human skin explants results in MVP release dependent upon PAFR signaling (10, 11).

Though increased MVP have been described in inflammatory disorders such as lupus erythematosus and psoriasis, the source of MVPs and overall pathologic significance are as yet unclear (12, 13). The present studies sought to define the metabolic pathway by which MVP are generated by the keratinocyte in response to UVB (UVB-MVP) and their significance in UVB-mediated effects. We also report that MVP derived from keratinocytes express the calcium-sensing receptor (14, 15), which allows us to test complex mixtures for keratinocyte-derived MVP.

RESULTS

To further confirm PAFR involvement in UVB-MVP release, HaCaT keratinocytes were treated with UVB or the metabolically stable PAFR agonist carbamoyl-PAF (CPAF) which resulted in increased MVP levels in cellular supernatant as soon as two hours post-treatment (Figure 1 a). Similar findings were noted in immortalized N/TERT and primary human keratinocytes (Supplementary Figure 1). Highest fluences of UVB employed resulted in only about 20% cell death (Supplementary Figure 2). As signal transduction pathways that regulate MVP release including p38 MAPK, ERK, NF-κB are downstream of PAFR activation (16-18), we next tested pharmacologic inhibitors of these pathways for their abilities to modulate UVB- and CPAF-mediated MVP release in HaCaT keratinocytes. Inhibitors of the p38MAPK, ERK, and the NF-κB pathways all attenuated stimulated MVP release (Figure 1 b), supporting the concept that PAFR signaling mediates UVB-MVP release. Yet the pan-caspase inhibitor Z-VAD-FMK exerted no effect on stimulated MVP release suggesting that apoptosis may not be involved. Ex vivo studies demonstrate that UVB exhibited similar MVP release responses in human skin explant tissue (Figure 1 c). Dosage- and time-response studies in wild-type (C57BL/6) mice further revealed that UVB induces MVP release in a dosage- and time-dependent manner with the maximal skin UVB-MVP released around 4 to 8 hours post UVB exposure (Figure 2 a, b).

The stimulus-mediated translocation of the enzyme acid sphingomyelinase (aSMase) from lysosomes to plasma membranes is a common lipid pathway mediating MVP

release (19, 20). Interestingly, PAFR activation has been reported to induce membrane translocation of aSMase and increase its enzymatic activity (21, 22). Several lines of evidence link aSMase as the effector for PAFR-mediated MVP release. First, HaCaT keratinocytes responded to CPAF and UVB with increased aSMase enzymatic activity (Supplementary Figure 3). Second, treatment with the aSMase inhibitor imipramine (23) post-UVB blocked stimulated MVP release in HaCaT cells (Figure 1 b), human skin explants (Figure 1 c) and murine skin (Figure 2 c). Finally, use of PAFR (*Ptafr-/-*) and aSMase (*Spmd1-/-*) KO mice confirmed the roles of PAFR and aSMase in UVB-MVP release in skin tissue (Figure 2 c). Topical application of the aSMase product C2 ceramide but not biologically inactive dihydroceramide (24) resulted in increased MVP in *Spmd1-/-* mice (Figure 2 c). These studies indicate that UVB generates MVP in a process involving PAFR signaling and aSMase.

An important knowledge gap in photobiology is how keratinocytes transmit UVB-generated signals systemically. To assess if UVB-MVP can potentially serve this role, we tested if keratinocyte-derived MVPs could be measured in plasma following UVB irradiation of skin. As shown in Figure 2 d, e, UVB irradiation of the back skin of wild-type mice resulted in increased levels of plasma MVP. Kinetics of plasma UVB-MVP closely resembled those of skin-derived UVB-MVP (compare Figures. 2 a, b with 2 d, e). To confirm the keratinocyte origin of the increased plasma MVPs, we tested the expression of membrane protein calcium-sensing receptor (CaSR), which has been demonstrated to be expressed in keratinocytes and other epithelial tissues (25). Immunocytochemistry studies (Supplementary Figure 4) confirmed that HaCaT and

epithelial KBP but not fibroblast cells were CaSR-positive. Flow-cytometry analysis revealed MVPs released from HaCaT and N/TERT were positive, yet fibroblasts and endothelial cells were negative for the CaSR (Supplementary Figure 5). Ex vivo studies using vacuum-generated blisters on human skin explants treated with UVB or topical CPAF (11) generated increased numbers of CaSR-positive MVPs in blister fluid comparison to control (Supplementary Figure 6), suggesting that a significant source of increased MVP in the blister fluid was from epidermal keratinocytes. These studies indicate that the CaSR can be used as a marker to track keratinocyte-derived MVPs. Murine plasma MVPs measured post-UVB expressed CaSR protein in a similar dose-dependent pattern as observed with cutaneous MVP release (Supplementary Figure 7) consistent with the notion that some of these blood MVPs were derived from epidermal keratinocytes following UVB irradiation.

We next confirmed the UVB effects on systemic MVP release in human subjects. As shown in Figure 3 a and Supplementary Table 1, pilot studies testing the effect of acute UVB on human skin in vivo demonstrate a two-fold increase in MVPs in skin biopsies 4 hours post-treatment following a clinically relevant (1000 J/m^2 UVB which is approximately 2.5x minimal erythema dose for subjects with Fitzpatrick types I and II phototypes) UVB fluence. To test if UVB irradiation of large surface areas of human skin results in systemic UVB-MVPs, we enrolled subjects undergoing medical phototherapy using a narrow band (311nm) UVB source in our dermatology clinic. Blood plasma MVPs were quantified before, two- and four-hours post-treatment. As depicted in Figure 3 b and Supplementary Table 2, subjects undergoing high-dose UVB treatments

exhibited an almost three-fold increase in MVP levels in plasma at 4 hours post-treatment. Flow cytometric analysis of plasma MVPs revealed that these subcellular bodies did not express appreciable levels of CaSR at baseline, yet, post-UVB a population of CaSR-positive MVPs were detected (see Figure 3 c). These studies employing both preclinical and human models indicate that UVB-MVPs derived from keratinocytes can be demonstrated systemically.

Given that UVB irradiation stimulates the release of bioactive lipids and protein cytokines (6, 7), we tested MVP derived from HaCaT keratinocytes treated with CPAF or UVB for the presence of 27 cytokines. As shown in Figure 4 a for a group of representative cytokines and Supplementary Table 3 for all the cytokines tested, most cytokines in UVB-MVPs were very low compare to unstimulated MVPs. Of note, levels of IL-1 receptor antagonist, a cytokine with anti-inflammatory properties (26), were elevated in UVB-MVPs.

UVB also generates PAF and oxidized glycerophosphocholine PAFR agonists (27). To assess whether PAFR agonistic lipids could also be found in keratinocyte-derived MVPs, we tested the PAFR biochemical agonistic activity of UVB-treated HaCaT keratinocytes. PAFR agonist levels in the lipid extracts derived from cell vs supernatant at various times post-UVB treatment were measured by exposing the lipid extracts to PAFR-positive KBP cells and measuring IL-8 release as a surrogate for PAFR activation, a validated biochemical assay that measures total PAFR activity (28-31). As

shown in Figure 4 b, at 5- and 10-min post UVB irradiation, the majority of PAFR agonistic activity (normalized to CPAF-induced IL-8 production in KBP cells) was cell-associated. However, by 120 min post irradiation, the only appreciable PAFR agonistic activity was found in the supernatants. To define whether the supernatant-associated PAFR activity was due to MVPs, we separated MVPs from the supernatants and tested each. The majority of the PAFR agonistic activity resided in MVPs, not MVP-depleted supernatants (Figure 4 c). The PAFR agonistic activity in UVB-MVP lipid extracts at 120 min was measured in comparison to various concentrations of a major PAF species (1-hexadecyl 2-acetyl GPC), which revealed the equivalent of approximately 18 ng PAF in 5 x 10^{10} MVPs (Supplementary Figure 8). To confirm the PAFR biological activity of MVP, we topically treated the dorsal ears of wild-type and PAFR KO mice with lipid extracts from UVB-irradiated HaCaT MVPs which resulted in increased ear thickness selectively in wild-type mice (Supplementary Figure 9). Finally, we removed MVP from plasma of UVB-treated wild-type vs *Spmd1-/-* mice and found that only UVB-MVP from wild-type mice contained PAFR activity (Supplementary Fig. 10). These studies support the concept that UVB-MVPs contain functional PAF agonists and fit with our hypothesized model in Figure 4 d that PAF agonists being generated in response to UVB residing in the cellular membranes activate the PAFR which translocate aSMase resulting in MVP which then carry the PAF lipids. We propose PAFR agonistic lipids are preserved in the MVPs, whereas acetylhydrolases remaining in the cell inactivate cell-associated PAF.

Given our findings that UVB-MVP carry PAFR agonists and leave the epidermis, we next tested whether these novel effectors mediate the systemic immunosuppressive response ascribed to PAFR activation (3-7). To assess the UVB-MVP effects on immune competence, wild-type or *Ptafr-/-* or *Spmd1-/-* mice received an immunosuppressive dose of UVB (7,500 J/m^2), intraperitoneal injection of CPAF, or control treatments and were then subjected to a well-established delayed-type hypersensitivity protocol (5, 30, 31). As expected, both UVB irradiation of skin and systemic exposure to CPAF resulted in immunosuppressive responses (as measured by inhibition of the ear thickness responses after elicitation with neoantigen DNFB) in wild-type mice. However, UVB did not generate immunosuppressive responses in *Ptafr-/-* nor in *Spmd1-/-* mice (Figure 5 a and Supplementary Figure 11). The ability of intraperitoneal injections of CPAF to attenuate the DNFB elicitation responses in the *Spmd1-/-* mice indicates that these mice retain their ability to respond to PAFR-mediated immunosuppressive effects. Inhibition of skin MVP release by the topical treatment of aSMase inhibitor imipramine on wild-type mouse skin showed similar inhibitory effects as in *Spmd1-/-* mice (Figure 5 b and Supplementary Figure 12), suggesting that skin-released MVPs were involved in UVB-induced immunosuppression. Topical imipramine did not attenuate CPAF-induced immunosuppressive effects. Systemic immunosuppression from various pro-oxidative stressors such as UVB involves upregulation of cytokines IL-10 and TGFβ, with decreased IL-12 and IFNγ and increased Treg differentiation (4-7). Thus, to confirm the functional testing we assayed these critical cytokines and Treg levels in lymph nodes following UVB in *Foxp3^{EGFP}* mice (31). As shown in Figure 5 c, UVB generated

increased mRNA levels of IL-10, TGF-β and the Treg-associated gene Foxp3 as well as the marker EGFP in the *Foxp3*^{EGFP} mice. UVB similarly downregulated Th1 cytokines IL-12A and IFN-γ in draining lymph nodes. It should be noted that expression of all of these genes were normalized by application of topical aSMase inhibitor imipramine.

DISCUSSION

The current report indicates that bioactive MVPs are released from keratinocytes within hours of exposure to biologically relevant UVB fluences. Discovery of a keratinocyte-selective MVP marker CaSR revealed UVB-MVPs can be found in the blood stream. The selectivity of the CaSR for the keratinocyte is modest, as other epithelial cell types (e.g., renal epithelium) also express this membrane protein (25). Yet in the present studies the increased levels of plasma MVP CaSR expression following UVB in mice (Supplementary Figure 7) and in human subjects (Figure 3 c) undergoing UVB treatments to widespread areas of skin fit with the concept that these MVP are keratinocyte-derived. Of interest, MVP derived from homogeneous cultures of keratinocytes do not result in 100% expression of the CaSR (see Supplementary Figure 5), which could result in an under estimation of keratinocyte-derived MVP when assayed in biologic specimens. Hence, the CaSR does have some limitations as a marker for keratinocyte MVP.

The present studies demonstrated that these subcellular particles carry both cytokines as well as the bioactive lipid PAF. Of interest, one of the cytokines that appears to be

upregulated in UVB-MVP is IL-1 receptor antagonist, a cytokine with well-known anti-inflammatory characteristics (26). The role of this cytokine in UVB responses is at present unclear, though theoretically it could be involved in the therapeutic effects of phototherapy. With our discovery that UVB-MVP contain PAFR agonistic activity, the focus of the current studies was to define the role of PAF transported by these subcellular particles. Use of both pharmacologic and genetic strategies aimed at the critical MVP-generating enzyme aSMase and the PAFR suggest that PAF carried in UVB-MVPs mediates delayed systemic immunosuppression responses. Details from preclinical studies indicate that the relevant PAFR for this immunosuppressive response is on the mast cell (4-6). Hence, a logical interpretation of the present findings is that metabolically labile PAF travels from the epidermal keratinocyte to the mast cell via MVP. As UVB-mediated systemic immunosuppression plays a role in diverse areas from carcinogenesis to treatment of pro-inflammatory disorders (4, 6, 7), the current mechanistic studies have clinical relevance. In summary, these studies provide new insights into how keratinocytes transfer environmental signals systemically and provides potential therapeutic targets for addressing adverse effects of UVB radiation exposure.

METHODS

Chemicals/UVB

All chemicals were obtained from Sigma-Aldrich unless indicated otherwise. Phorbol ester 12-O-Tetradecanoylphorbol-13 acetate (TPA) was used in cell lines/skin explants/mice as a PAFR-independent stimulus as TPA does not generate PAF in our

model systems (28, 29, 31). UVB of cells/skin explants/mice and human arms used a Philips F20T12/UVB lamp source (Somerset, NJ) using Kodacel filter to remove UVC (27, 28). The fluences used were based upon previous studies by our group and others. In particular, for keratinocyte cell lines in vitro, fluences above 1.8 kJ/m^2 were needed to generate MVP (10, 28). In addition, for human skin, fluences of 1.0 kJ/m^2 are needed to generate MVP (11). This is an approximate fluence reported to generate immunosuppression on human skin (32). Finally, using mice on a C57BL/6 background, UVB fluences of at least 5 kJ/m^2 are needed to induce systemic immunosuppression (3, 5). Human phototherapy studies used a Daavlin nUVB UV 7 Series source (Bryan, OH)

Cell culture

Cell lines were grown as previously described (10, 17, 27). The HaCaT keratinocyte-derived cell line (provided by Dr. Petra Boukamp at the German Cancer Research Center, Heidelberg, Germany), and PAFR-positive KBP and control (PAFR-negative) KBM cells generated as described (29) were grown in DMEM high glucose media with 10% FCS. N/TERT and primary keratinocytes were grown in EpiLife medium with Human Keratinocyte Growth Supplement. KBP/KBM cells were grown to 40% confluence, and HaCaT cells were grown to approximately 80-90% confluence in 10 cm dishes, and washed three times with Hanks Balanced Salt Solution (HBSS) and then incubated with HBSS + 10 mg/ml fatty acid-free BSA for UVB exposures. Cells were treated with either no treatment, vehicle (0.1% Ethanol), CPAF (100 nM), Imipramine (50 μM) pre- and post-UVB radiation, 3,600 J/m^2 UVB if not specifically mentioned. In

some experiments TPA (100 nM) , or 10 μM of the inhibitors p38 MAPK inhibitor SB203580 (4-[4-(4-fluorophenyl)-2-(4-methylsulfinylphenyl)-1H-imidazol-5-yl] pyridine), Erk1/2 (MAPK/ERK kinase [MEK] inhibitor PD98,059), NF-kB inhibitor ammonium pyrrolidine dithiocarbamate (PDTC) or pan-caspase inhibitor (Z-VAD-FMK (carbobenzoxy-valyl-alanyl-aspartyl-[O-methyl]-fluoromethylketone; 24 μM) were given 1 hour pre-CPAF treatment (except for imipramine which was given post-UVB). The MAPK and NFκB inhibitor doses were from our previous studies which have demonstrated select inhibition of respective pathways (17, 28). The concentration of Z-VAD-FMK used was based upon its ability to block UVB-mediated apoptosis in HaCaT cells (ref 28 and *data not shown*). None of the chemicals used except for imipramine absorbed appreciably in the UVB spectrum.

Mice

All studies involving mice were approved by the Wright State University Laboratory Animal Review Board. Female C57BL/6-wild type mice (PAF-R expressing; age 6-8 week) were purchased from The Charles River Laboratories and we also used some male and female wild-type mice from our own colonies. The PAFR KO (*Ptafr*-/-) mice on a C57BL/6 background were a kind gift from Professor Takao Shimizu at University of Tokyo. The *Spmd1* +/- heterozygous mice originally from Dr. Edward Schuchman's laboratory (19) were obtained from Dr. Irina Petrache's group at the National Jewish Medical Center in Denver Colorado. The aSMase KO (*Spmd1* -/-) mice were bred by heterozygous littermates. Foxp3^{EGFP} knockin transgenic mice on the C57BL/6

294 background (age 8-12 wk) were procured from The Jackson Laboratory as previously
295 reported (31). All lines were re-derived every two years. All mice were housed under
296 specific pathogen-free conditions and all procedures were approved by the Institutional
297 Animal Care and Use Committee of Wright State University. Mice were intraperitoneal
298 injected with ketamine/ xylazine (100 and 10mg/kg, respectively), shaved, then treated
299 with either no treatment, vehicle (90% DMSO+10% ethanol), imipramine (500 μM), UVB
300 (7,500 J/m^2), imipramine immediately after UVB treatment. After treatment for 4 hours,
301 mice were euthanized. Skin was collected by 6 mm punch biopsies. Tissues were cut
302 up finely in the microcentrifuge tube and digested in 0.5 ml of 5 mg/ml collagenase and
303 dispase solution overnight 37 °C for MVP isolation. Blood was collected from heart in
304 heparin coated tubes and the blood plasma prepared immediately for MVP isolation.
305

306 **Human skin explants**

307 De-identified discarded skin was obtained from human contouring (abdominoplasty and
308 brachioplasty) surgeries (11, 28). Skin explants were washed, fat trimmed, and placed
309 in PBS warmed at 37°C, then treated with either no treatment, 100 μl per 1 x 1 cm^2 area
310 of vehicle (90% DMSO+10% ethanol), imipramine (500 μM), UVB (2,500 J/m^2),
311 imipramine 1 hour before UVB or immediately after UVB treatment. After 4 hours, skin
312 was harvested by punch biopsies. Tissue samples were digested with
313 collagenase/dispase solution overnight for MVP isolation (11, 28).
314

315 **Human subject skin and blood preparation**

All studies involving humans were approved by the Wright State University Institutional Review Board, Dayton Ohio and followed the Declaration of Helsinki Principles. Volunteers provided written informed consent before enrollment. For skin MVP collection, healthy donors were irradiated with 1000 J/m^2 UVB using our Philips F20T12/UVB lamp source on arm skin. After 4 hours, skin tissue were biopsied (5 mm punch biopsies) from irradiated and non-irradiated areas for MVP isolation. For blood plasma MVP, patients who were on a stable dose of narrow-band UVB phototherapy (over 20 treatments; with last UVB treatment at least 4 days before the current treatment) were enrolled in this study. Blood was drawn before, two- and four-hours post-treatment of subjects undergoing a phototherapy treatment of at least 80% body surface area using a Daavlin nUVB source (Bryan, OH) to entire body (except in groin area) in heparin-coated tubes and proceeded immediately for MVP isolation.

MVP isolation and analysis

MVP were isolated from culture medium, skin biopsies and blood plasma as previously reported (10, 11, 28). In brief, cell culture medium, skin biopsy lysate and blood plasma were collected and centrifuged at 2,000 *x g* for 20 minutes at 4 °C to remove cells and debris. Skin biopsy tissue and blood plasma then followed with 20,000 *x g* centrifugation for 10 minutes at 4 °C to remove remaining tissue and subcellular component. MVP were then pelleted after 20,000 *x g* centrifugation at 70 minutes at 4°C from the sample supernatant. In some experiments exosomes were collected by use of an additional 170,000 *x g* centrifugation for 90 minutes. The concentrations of the MVP/exosomes were determined by using a NanoSight NS300 instrument (NanoSight Ltd, Malvern

Instruments, Malvern, UK). Three 30-second videos of each sample were recorded and analyzed with NTA software version 3.0 to determine the concentration and size of measured particles with corresponding standard error. As shown in Supplementary Figure 13, MVP were characterized by western blotting as expressing Annexin V with only low levels of exosome specific markers CD63 and Tsg 101. Moreover, transmission electron microscopy revealed MVP with appropriate dimensions (Supplementary Figure 13).

Flow cytometry

MVPs were aliquoted into microcentrifuge tubes with similar concentrations. Each tube was stained with either 1 ng isotype control or 1 ng CaSR-FITC antibody (Novus Biologicals Catalog NB100-1830F) Samples were cultured in the dark at 4°C for 45 minutes. CaSR expression in MVP were analyzed by Bd Accuri C6 Flow Cytometer (BD Biosciences, New Jersey, USA). Percentage of CaSR-positive MVPs were derived by comparison of CaSR- stained MVPs to isotype control-stained MVPs.

Measurement of cytokines and chemokines

HaCaT keratinocytes were treated with vehicle (0.1% ethanol), CPAF (100 nM) or UVB (3,600 J/m^2), and after 4 hours, medium was collected for MVP isolation. MVP were re-suspended with 100 μl filtered PBS and stored in -80 °C before assay. Cytokine levels were measured by Bio-Plex ProTM Human Cytokine 27-plex Assay kit (Bio Rad) as

previously reported (28). Cytokine concentration (pg/ml) was normalized to MVP number for analysis.

Measurement of PAFR agonistic activity

The presence and quantitation of PAFR agonists in lipid extracts derived from HaCaT keratinocytes and from MVP isolated from murine plasma was assessed by the ability of lipid extracts to induce IL-8 release in PAFR-expressing KBP cells, but not in PAFR-deficient KBM cells as previously reported (28, 31). KB cells were originally derived from a patient with a nasopharyngeal carcinoma. These cells are a model for human keratinocytes yet lack PAFRs. The KB cells (obtained from American Type Culture Collection) were transduced with the MSCV2.1 retrovirus containing the PAF-R (KBP). Control cells (KBM) were transduced with the empty MSCV2.1 retrovirus (29). Lipid extracts (33) were isolated either from UVB treated HaCaT cells, or total cell medium at various time points and HaCaT induced MVP or MVP-depleted supernatant at 2 hours. Lipids were added to PAFR-expressing KBP cells and supernatants removed at 4 hours. The ratio of IL-8 released by treated KBP cells was compared to 1 nM CPAF positive control- treated KBP cells were used to determine the PAFR agonistic activity level. Some experiments tested these lipid extracts derived from MVP on PAFR-negative KBM cells using TPA as a positive control for IL-8 release (10, 28, 30).

Contact Hypersensitivity (CHS) studies

The CHS study followed by the protocol previously reported (5, 30, 31). Briefly, at day 0, both Wild-type, *Ptafr-/-* and *Spmd1 -/-* mice were treated with either no treatment, CPAF (250 ng i.p. injection), histamine (1 μg sc for *Ptafr-/-*) or UVB (7,500 J/m^2), or to an area of 2.5 x 2.5 cm on lower back skin which hair had been removed using clippers 24 hours previously, and had surrounding skin blocked off using heavy black paper. Five days later, non-irradiated upper back/shoulder skin (that had been previously shielded from UVB using heavy opaque paper) was treated with 50 μl of 0.5% dinitrofluorobenzene (DNFB) in 4:1 acetone:olive oil (*v:v*). Nine days post-DNFB treatment, murine ear thickness was recorded, then one ear was be treated with 10 μl of 0.5% DNFB and one ear treated with vehicle alone. Murine ear thickness was recorded again after 24 hrs. The immunosuppressive effects will be determined by the ear thickness changes between DNFB- and vehicle-treated ears. Controls without the sensitization step revealed less than a 5% change in ear thickness from the DNFB treatment. Histamine was used as a positive control in the PAFR KO mice as per our previously reported findings (5, 31).

Real-time PCR

Cytokines and Treg expressions of *Foxp3^{EGFP}* mice skin draining lymph nodes were analyzed by Real-time PCR exactly as previously described (31). Total mRNA was purified from mice skin draining lymph nodes using the RNeasy Micro Kit (Invitrogen). cDNA was synthesized using iScript Supermix (Bio-Rad), and then real-time PCR analysis was performed using Advanced SYBR green supermix (Bio-Rad) according to

the manufacture`s protocol. Normalization of mRNA expression was performed based on the expression of β-Actin utilizing cycling threshold (ΔCT) method and the amount of PCR product was calculated based on $2^{-\Delta\Delta CT}$. See Supplemental Methods for PCR primer sequences.

Statistics

All statistical calculations were performed using GraphPad Prism Version 6.0 software. Statistical significance was determined by 2-sided student t test or One-way ANOVA with post-hoc Holm-Sidak test with alpha=5%. A p value < 0.05 was considered significant.

Acknowledgements

This research was supported in part by grants from the National Institutes of Health grant R01 HL062996 (JBT), ES031087 (JBT + YC), GM130583 (MGK), R21 AR071110 (JCB), Veteran's Administration Merit Award 5I01BX000853 (JBT). The content is solely the responsibility of the authors and does not necessarily represent the official views of the National Institutes of Health or the US Veterans Administration.

Competing Interests

The authors declare no competing interests.

Author Contributions

L.L., C.R., C.K., E.E.C., D.R.C., R.P.S., J.C.B., Y.C., M.G.K., J.B.T. designed the studies.

425 L.L., A.A.A., K.E.F., P.T., C.B., B.W., C.M., B.S., Z.S., C.R., A.R.W., E.E.C., L.E.K.,
426 D.R.C., R.P.S., J.W., C.M.R., M.G.K, J.B.T. performed experiments. L.L., K.E.F., J.C.B.,
427 Y.C., D.R.C, C.K., J.B.T. were involved in data analysis. B.W., A.R.W., C.M., B.S., Z.S.,
428 C.R., E.E.C., C.K, R.M.J., J.B.T. were involved in collecting human subject samples.
429 J.B.T. supervised the study. L.L., J.B.T. wrote the manuscript.

430

References

1. Liu-Smith F, et al. UV-Induced Molecular Signaling Differences in Melanoma and Non-melanoma Skin Cancer. *Adv Exp Med Biol.* 2017;996:27-40.
2. Madan V, et al. Non-melanoma skin cancer. *Lancet.* 2010;375(9715):673-85.
3. Walterscheid JP, et al. Platelet-activating factor, a molecular sensor for cellular damage, activates systemic immune suppression. *J Exp Med.* 2002;195(2):171-9.
4. Damiani E, and Ullrich SE. Understanding the connection between platelet-activating factor, a UV-induced lipid mediator of inflammation, immune suppression and skin cancer. *Prog Lipid Res.* 2016;63:14-27.
5. Ocana JA, et al. Platelet-Activating Factor-Induced Reduction in Contact Hypersensitivity Responses Is Mediated by Mast Cells via Cyclooxygenase-2-Dependent Mechanisms. *J Immunol.* 2018;200(12):4004-11.
6. Bernard JJ, et al. Photoimmunology: how ultraviolet radiation affects the immune system. *Nat Rev Immunol.* 2019;19(11):688-701.
7. Tse BCY, and Byrne SN. Lipids in ultraviolet radiation-induced immune modulation. *Photochem Photobiol Sci.* 2020;19(7):870-8.
8. Tickner JA, et al. EV, Microvesicles/MicroRNAs and Stem Cells in Cancer. *Adv Exp Med Biol.* 2018;1056:123-35.
9. Lane RE, et al. Extracellular vesicles as circulating cancer biomarkers: opportunities and challenges. *Clin Transl Med.* 2018;7(1):14.
10. Bihl JC, et al. UVB Generates Microvesicle Particle Release in Part Due to Platelet-activating Factor Signaling. *Photochem Photobiol.* 2016;92(3):503-6.
11. Fahy K, et al. UVB-generated Microvesicle Particles: A Novel Pathway by Which a Skin-specific Stimulus Could Exert Systemic Effects. *Photochem Photobiol.* 2017;93(4):937-42.
12. Beyer C, and Pisetsky DS. The role of microparticles in the pathogenesis of rheumatic diseases. *Nat Rev Rheumatol.* 2010;6(1):21-9.
13. Pelletier F, et al. Increased levels of circulating endothelial-derived microparticles and small-size platelet-derived microparticles in psoriasis. *J Invest Dermatol.* 2011;131(7):1573-6.
14. Tu CL, et al. The extracellular calcium-sensing receptor is required for calcium-induced differentiation in human keratinocytes. *J Biol Chem.* 2001;276(44):41079-85.
15. Owen JL, et al. The role of the calcium-sensing receptor in gastrointestinal inflammation. *Semin Cell Dev Biol.* 2016;49:44-51.
16. Zhang Y, et al. RGS16 attenuates galphaq-dependent p38 mitogen-activated protein kinase activation by platelet-activating factor. *J Biol Chem.* 1999;274(5):2851-7.
17. Marques SA, et al. The platelet-activating factor receptor activates the extracellular signal-regulated kinase mitogen-activated protein kinase and induces proliferation of epidermal cells through an epidermal growth factor-receptor-dependent pathway. *J Pharmacol Exp Ther.* 2002;300(3):1026-35.
18. Tran TV, et al. Blockade of platelet-activating factor receptor attenuates abnormal behaviors induced by phencyclidine in mice through down-regulation of NF-κB. *Brain Res Bull.* 2018;137:71-8.

19. Bianco F, et al. Acid sphingomyelinase activity triggers microparticle release from glial cells. *EMBO J.* 2009;28(8):1043-54.
20. Record M, et al. Extracellular vesicles: lipids as key components of their biogenesis and functions. *J Lipid Res.* 2018;59(8):1316-24.
21. Goggel R, et al. PAF-mediated pulmonary edema: a new role for acid sphingomyelinase and ceramide. *Nat Med.* 2004;10(2):155-60.
22. Lang PA, et al. Stimulation of erythrocyte ceramide formation by platelet-activating factor. *J Cell Sci.* 2005;118(Pt 6):1233-43.
23. Liangpunsakul S, et al. Imipramine blocks ethanol-induced ASMase activation, ceramide generation, and PP2A activation, and ameliorates hepatic steatosis in ethanol-fed mice. *Am J Physiol Gastrointest Liver Physiol.* 2012;302(5):G515-23.
24. Goni FM, et al. Biophysical properties of sphingosine, ceramides and other simple sphingolipids. *Biochem Soc Trans.* 2014;42(5):1401-8.
25. Leach K, et al. International Union of Basic and Clinical Pharmacology. CVIII. Calcium-Sensing Receptor Nomenclature, Pharmacology, and Function. *Pharmacol Rev.* 2020;72(3):558-604.
26. Dinarello CA. The IL-1 family of cytokines and receptors in rheumatic diseases. *Nat Rev Rheumatol.* 2019;15(10):612-32.
27. Marathe GK, et al. Ultraviolet B radiation generates platelet-activating factor-like phospholipids underlying cutaneous damage. *J Biol Chem.* 2005;280(42):35448-57.
28. Liu L, et al. Thermal Burn Injury Generates Bioactive Microvesicles: Evidence for a Novel Transport Mechanism for the Lipid Mediator Platelet-Activating Factor (PAF) That Involves Subcellular Particles and the PAF Receptor. *J Immunol.* 2020;205(1):193-201.
29. Pei Y, et al. Activation of the epidermal platelet-activating factor receptor results in cytokine and cyclooxygenase-2 biosynthesis. *J Immunol.* 1998;161(4):1954-61.
30. Zhang Q, et al. Staphylococcal lipoteichoic acid inhibits delayed-type hypersensitivity reactions via the platelet-activating factor receptor. *J Clin Invest.* 2005;115(10):2855-61.
31. Sahu RP, et al. Cigarette smoke exposure inhibits contact hypersensitivity via the generation of platelet-activating factor agonists. *J Immunol.* 2013;190(5):2447-54.
32. Matthews YJ, et al. A UVB wavelength dependency for local suppression of recall immunity in humans demonstrates a peak at 300 nm. *J Invest Dermatol.* 2010;130(6):1680-4.
33. Bligh EG, and Dyer WJ. A rapid method of total lipid extraction and purification. *Can J Biochem Physiol.* 1959;37(8):911-7.

Figures and Legends

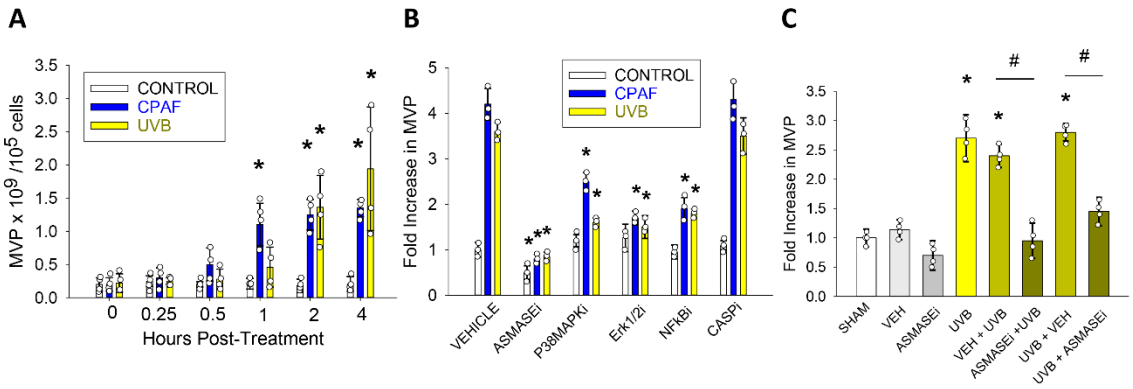

Figure 1. UVB-induced MVP release in HaCaT keratinocytes and human skin explant tissue. *In vitro studies*: **a**) HaCaT keratinocytes were treated with 0.1% ethanol vehicle control, 100 nM CPAF or 3,600 J/m^2 UVB and the levels of MVPs released into supernatants measured at various times. **b**) HaCaT keratinocytes were treated with CPAF, UVB and inhibitors of aSMase (imipramine, 50 μM), P38 MAPK (SB 203580; 10 μM), ERK ½ (PD 98,059; 10 μM), NF-κB (PDTC; 10 μM), or pan-caspase (Z-VAD-FMK, 24 μM) 1 hour before CPAF/UVB or immediately post-UVB (imipramine) treatments. Levels of MVPs released into supernatants were measured at 4 hours. **c**) *Ex vivo studies*: Human skin explants were treated with no treatment, vehicle (90% ethanol + 10% DMSO), 500 μM aSMase inhibitor imipramine, 2,500 J/m^2 UVB, imipramine/vehicle 30 minutes before UVB or immediately following UVB irradiation. 4 hours later MVPs were quantified in skin biopsies. The data in **a-c** are mean ± SD of three (**b**) or four (**a**,**c**) independent experiments. Statistically significant differences were determined using One-way ANOVA test. *p < 0.05 vs. control (**a**), vehicle (**b**) or sham (**c**). #p < 0.05.

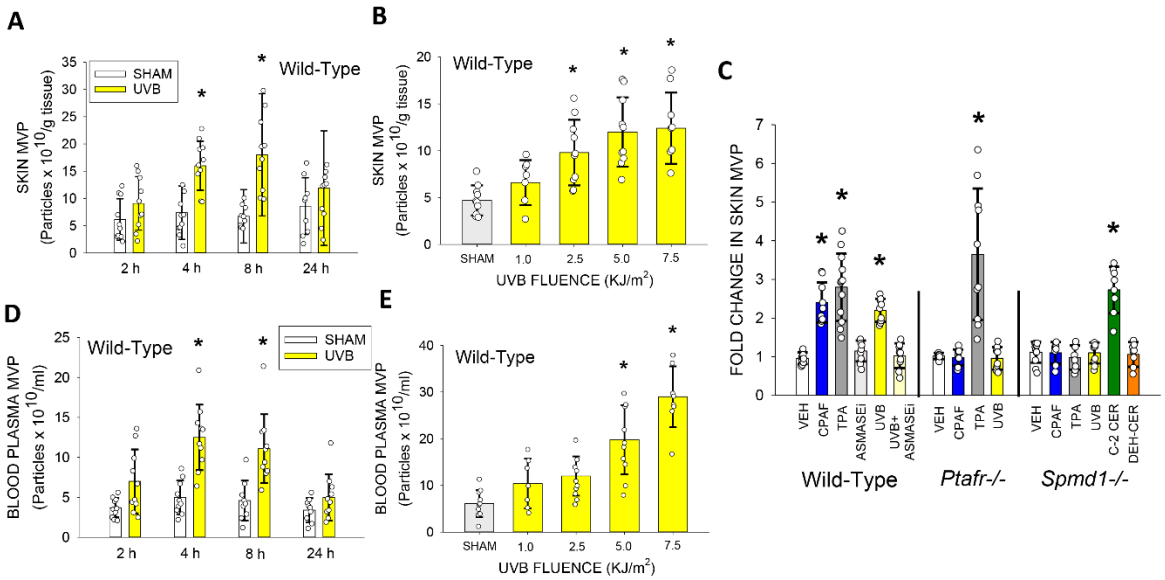

Figure 2. UVB-induced MVP release requires PAFR activation and aSMase. Groups of 7-10 wild-type mice were treated with sham or 7,500 J/m^2 UVB for various times, MVPs were quantified in **a)** skin tissue and **d)** blood plasma. Groups of 8-10 wild-type mice were treated with various UVB fluences and 4h later MVPs were quantified in **b)** skin tissue and **e)** blood plasma. **c**) Groups of 8-12 wild-type, PAFR- and aSMase-deficient mice were treated with sham, UVB (7,500 J/m^2), vehicle (90% ethanol + 10% DMSO), CPAF (100 μM), TPA (100 μM), C2 ceramide (20 μM), or inactive dihydroceramide (20 μM) and 4 hours later duplicate skin biopsies performed, weighed, and MVP quantitated. Data are mean ± SD. Statistically significant differences were determined using One-way ANOVA test. *p < 0.05 vs. sham (**a, b, d, e**) or vehicle (**c**).

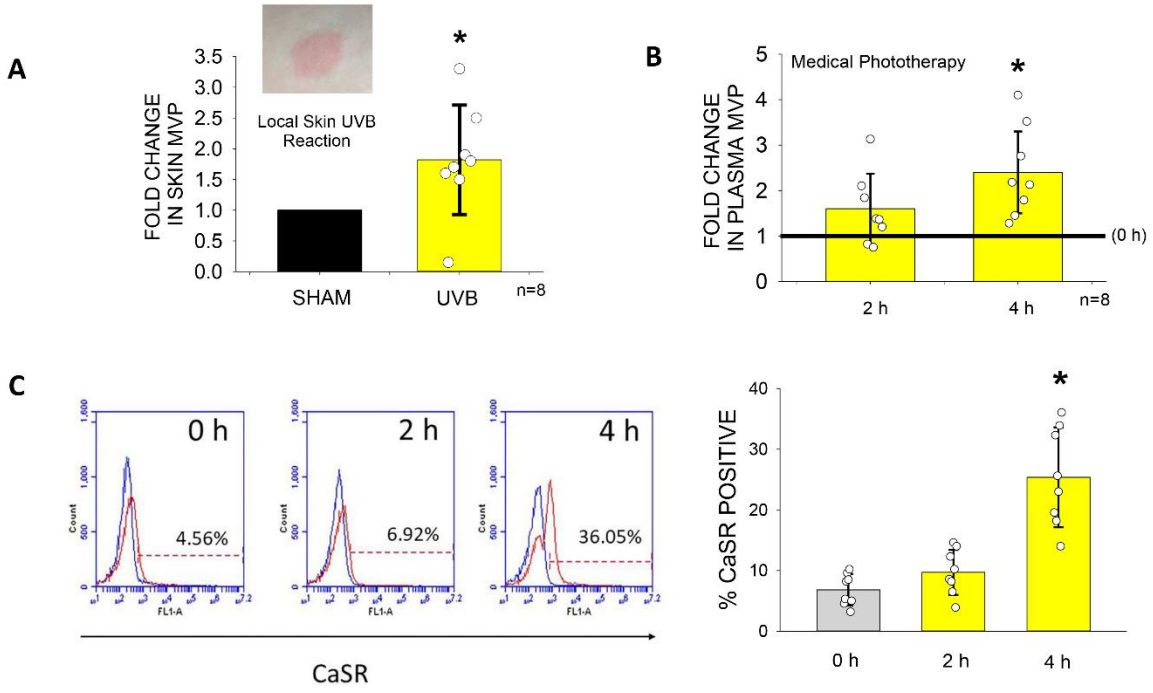

Figure 3. UVB-MVPs are released in human skin and blood plasma. a) A group of eight human subjects (see Supplementary Table 1) were exposed with 1000 J/m^2 UVB on volar forearm, and 4 hours later, skin biopsies were collected on both UVB irradiated (see example of UVB skin reaction) and non-irradiated (SHAM) areas, weighed, and MVP measured. **b**) Blood samples were collected from 8 clinical patients receiving narrow-band UVB phototherapy (see Supplementary Table 2) at either before (0 h), 2 hours post- or 4 hours post-therapy. MVPs were isolated from blood plasma and quantified. **c**) CaSR expression on blood plasma MVPs (n = 8) were analyzed by flow cytometry. MVPs were stained with either isotype control (blue line) or CaSR antibody (red line). CaSR- positive MVPs were determined using flow cytometry by CaSR-stained MVPs excluding the isotype control stained MVPs. Quantification of CaSR expression flow cytometry data on blood plasma MVPs. Data are mean ± SD. Statistically significant differences were determined using 2-sided student t-test (**a**) or One-way ANOVA test (**b, c**). *p < 0.05 vs. sham (**a**), 0 h (**b, c**).

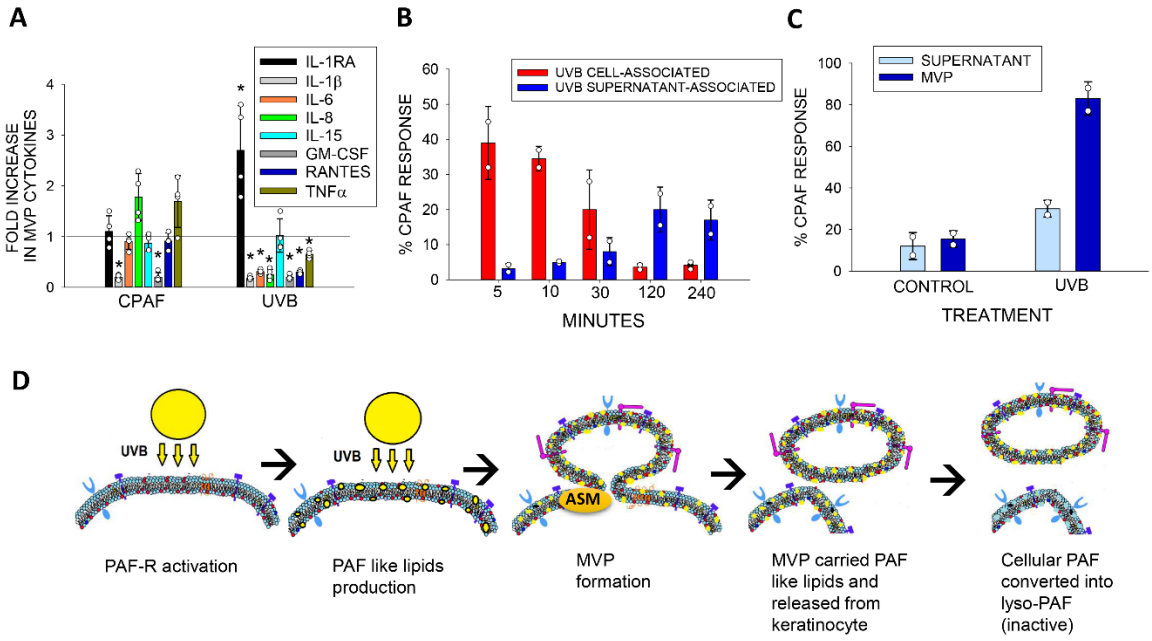

Figure 4. UVB-MVPs carry cytokines and PAF lipids. **a**) HaCaT keratinocytes were treated with 100 nM CPAF or 3,600 J/m^2 UVB. MVPs were isolated from cell supernatant 4 hours post-treatment and analyzed for cytokine expression using Bio-Plex Pro™ Human Cytokine 27-plex Assay kit. Data are mean ± SE of representative cytokines from 3 separate experiments (see Supplementary Table 3 for all cytokine values). *Denotes statistically significant ($p < 0.05$) differences from control using one-way ANOVA test. **b**) Lipids extracted from UVB-treated HaCaT keratinocytes and culture medium were collected at various times and tested for PAFR agonistic activity using PAFR+ KBP cell release of IL-8 in supernatant in comparison to 1 nM CPAF. **c**) HaCaT supernatants at 120 minutes post-UVB were separated into MVP and MVP depleted supernatant, and lipids extracted and then added to PAFR positive KBP cells to test the PAFR agonistic response. **b)** and **c)** are representative graphs using duplicate samples from three separate experiments with similar results. **d**) Hypothesized mechanism by which UVB generates PAFR agonists which activate the PAFR resulting in aSMase activation generating MVP which carry bioactive PAFR agonists, whereas cell-associated PAFR agonists are rapidly metabolized.

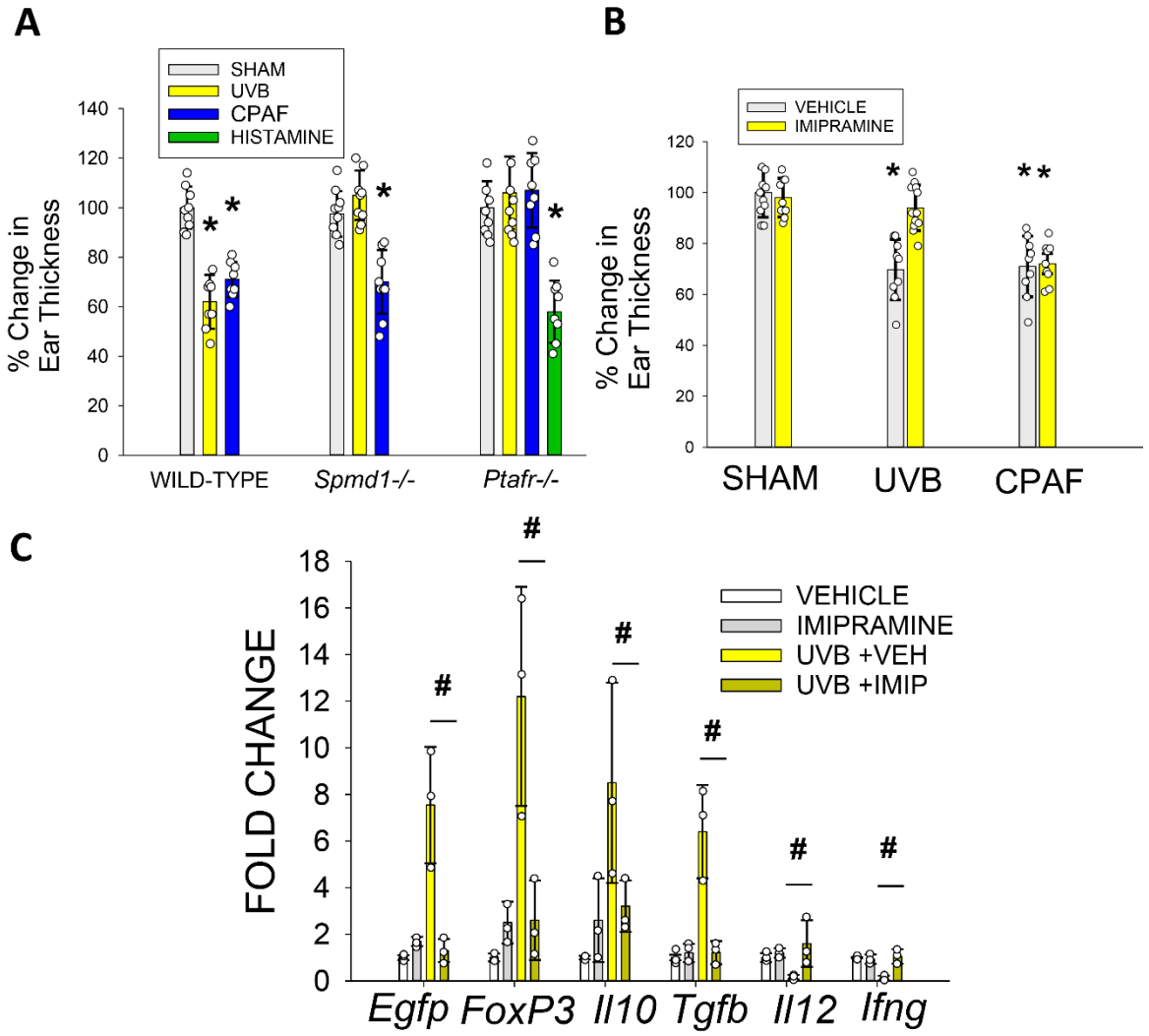

Figure 5. UVB-MVPs contribute to UVB induced immunosuppression. **a**) Groups of 8-10 wild-type mice, *Spmd1-/-* and *Ptafr-/-* were either injected with 250 ng CPAF i.p., 1 μg histamine s.c., or exposed to 7,500 J/m^2 UVB on shaved back. The mice then underwent sensitization with chemical DNFB on un-irradiated back skin followed by ear elicitation. **b**) Groups of 8-12 Wild-type mice were treated with UVB, CPAF and then treated with topical imipramine (500 μM) for 3 days. The mice then underwent sensitization with chemical DNFB on un-irradiated back skin followed by ear elicitation. For **a**) and **b**), decreased % of ear thickness change was indicated as a suppressed immune response compared to sham-treated mice. The data are the mean ± SD % changes in ear thickness compared to sham values. **c**) Groups of *FoxP3^{EGFP}* mice were treated with topical vehicle, imipramine, or 7,500 J/m^2 UVB followed immediately and daily x 3 of vehicle or imipramine. Draining lymph nodes were harvested at day 5 post-

606 UVB and subjected to RT-PCR. The data are the mean ± SD relative mRNA expression
607 of Foxp3, EGFP, IL-10, TGF-β, IL-12A, IFN-γ using groups of 3-4 mice repeated three
608 times. Statistically significant differences were determined using One-way ANOVA test.
609 *$p < 0.05$ vs. sham (**a**, **b**). #$p < 0.05$.